

**Zt and γt production via top flavour-changing
neutral couplings at the Fermilab Tevatron**

F. del Aguila, J. A. Aguilar-Saavedra
Departamento de Física Teórica y del Cosmos
Universidad de Granada
E-18071 Granada, Spain

Ll. Ametller
Dep. Física i Enginyeria Nuclear
Universitat Politècnica de Catalunya
E-08034 Barcelona, Spain

Abstract

Associated single top production with a Z boson or a photon at large hadron colliders provides a precise determination of top flavour-changing neutral couplings. The best way to measure these couplings with the up quark at Tevatron is to search for events with three jets and missing energy or events with a photon, a charged lepton, a jet and missing energy. Other decay channels are also discussed.

PACS: 12.15.Mm, 12.60.-i, 14.65.Ha, 14.70.-e

Large hadron colliders will be top factories, allowing to measure its properties very precisely. In contrast with its mass, which is the best known quark mass, top couplings are very poorly known [1]. In this Letter we point out that associated single top production with a Z boson or a photon is very sensitive to the flavour-changing neutral (FCN) couplings Vtq , with V a Z boson, a photon or a gluon and q a light quark u or c . These vertices are very small in the Standard Model (SM), being then an obvious place to look for new physics. Although top pair production gives large top samples, the leptonic Zt and γt signals become cleaner and statistically more significant with increasing energy and luminosity. At any rate, the determination of top FCN couplings from Zt and γt production has a comparable, if not a higher precision than from top decays as we will show here for Tevatron. On the other hand, both measurements have not only to be consistent but they will improve their statistical significance when combined together. In the following we concentrate on Runs I and II with integrated luminosities of 109 pb^{-1} and 2 fb^{-1} , respectively. The charm contribution to associated top production with a Z boson or a photon is

40 times smaller than the up contribution at Tevatron energies $\sqrt{s} = 1.8 - 2$ TeV. Hence, Tevatron is only sensitive in these production processes to top couplings with the up quark. This will not be the case at the CERN Large Hadron Collider (LHC), where the charm contribution becomes relevant. In any case there is no model-independent reason for the Vtu couplings to be small, and it is theoretically important to measure them precisely.

The most significant decay channels depend on the collider and luminosity. For Zt production, the $\nu\bar{\nu}jjb$ decay channel, with $Z \rightarrow \nu\bar{\nu}$ and $W \rightarrow q\bar{q}'$, gives the best determination of the Ztu couplings in both Tevatron runs. The $jjl\nu b$ mode, with $Z \rightarrow q\bar{q}$ and $W \rightarrow l\nu$, has a similar branching ratio but a larger background. For higher luminosity at Tevatron Run III or at the LHC, the leptonic mode $l^+l^-\nu b$, with both Z and W decaying leptonically, and the $b\bar{b}l\nu b$ mode are more significant. For γt production the $\gamma l\nu b$ channel, with $W \rightarrow l\nu$, gives a cleaner signal than the γjjb mode with $W \rightarrow q\bar{q}'$, allowing a better determination of the γtu vertex. This leptonic channel also gives the best limit on the gtu coupling. A detailed discussion of all these decay channels at LHC will be presented elsewhere [2]. Throughout this Letter we consider that the top quark decays predominantly into Wb [3], and we sum t and \bar{t} production.

The Lagrangian involving FCN couplings between the top, a light quark $q = u, c$ and a Z boson, a photon A or a gluon G^a can be written in standard notation as [4]

$$\begin{aligned}\mathcal{L} = & \frac{g_W}{2c_W} \bar{t} \gamma_\mu (X_{tq}^L P_L + X_{tq}^R P_R) q Z^\mu \\ & + \frac{g_W}{2c_W} \bar{t} (\kappa_{tq}^{(1)} - i\kappa_{tq}^{(2)} \gamma_5) \frac{i\sigma_{\mu\nu} q^\nu}{m_t} q Z^\mu \\ & + e \bar{t} (\lambda_{tq}^{(1)} - i\lambda_{tq}^{(2)} \gamma_5) \frac{i\sigma_{\mu\nu} q^\nu}{m_t} q A^\mu \\ & + g_s \bar{t} (\zeta_{tq}^{(1)} - i\zeta_{tq}^{(2)} \gamma_5) \frac{i\sigma_{\mu\nu} q^\nu}{m_t} T^a q G^{a\mu} + \text{h.c.},\end{aligned}\tag{1}$$

where $P_{R,L} = (1 \pm \gamma_5)/2$ and T^a are the Gell-Mann matrices satisfying $\text{Tr}(T^a T^b) = \delta^{ab}/2$. The $\sigma_{\mu\nu}$ terms are dimension 5 and absent at tree level in renormalizable theories like the SM. Hence, they are suppressed by one-loop factors $\sim \alpha/\pi$. Besides, in the absence of tree level FCN couplings they are also suppressed by the GIM mechanism. Thus, these terms are typically small in renormalizable theories. However, in scenarios with new dynamics near the electroweak scale effective couplings involving the t quark may be large. On the other hand, the γ_μ terms can be quite large in principle. Although rare processes require small FCN couplings between light quarks, the top can have relatively large couplings with the quarks u or c , but not with both simultaneously. In specific models FCN couplings scale with

the quark masses, but this is not general. Simple well-defined models extending the SM with vector-like fermions can be written fulfilling all precise electroweak data and saturating the inequalities

$$\begin{aligned} |X_{tu}^L| &\leq 0.28 \quad , \quad |X_{tu}^R| \leq 0.14, \\ |X_{tc}^L| &\leq 0.14 \quad , \quad |X_{tc}^R| \leq 0.16 \end{aligned} \tag{2}$$

at 90% C. L. [5]. It is usually expected that new physics, and in particular the mass generation mechanism, will show up first in the third family and thus in the top quark, and large hadron colliders are the best place to perform a precise measurement of these couplings. The present 95% C. L. limits on the top branching ratios at Tevatron are $\text{Br}(t \rightarrow Zq) \leq 0.33$, $\text{Br}(t \rightarrow \gamma q) \leq 0.032$ [3], $\text{Br}(t \rightarrow gq) \leq 0.15$ [6], which imply

$$\begin{aligned} X_{tq} &\equiv \sqrt{|X_{tq}^L|^2 + |X_{tq}^R|^2} \leq 0.84, \\ \kappa_{tq} &\equiv \sqrt{|\kappa_{tq}^{(1)}|^2 + |\kappa_{tq}^{(2)}|^2} \leq 0.778, \\ \lambda_{tq} &\equiv \sqrt{|\lambda_{tq}^{(1)}|^2 + |\lambda_{tq}^{(2)}|^2} \leq 0.26, \\ \zeta_{tq} &\equiv \sqrt{|\zeta_{tq}^{(1)}|^2 + |\zeta_{tq}^{(2)}|^2} \leq 0.15. \end{aligned} \tag{3}$$

Similar limits have been reported searching for $t\bar{q}$ production at LEP2 [7]. Relying on the same decays it has been estimated that LHC with a luminosity of 100 fb^{-1} and future linear colliders will eventually reduce these bounds to $X_{tq} \leq 0.02$, $\kappa_{tq} \leq 0.015$, $\lambda_{tq} \leq 0.0035$ [8, 9, 10, 11]. In Ref. [12] the limits on the strong top FCN couplings have been studied looking at the production of a single top quark plus a jet at hadron colliders, obtaining $\zeta_{tu} \leq 0.029$, $\zeta_{tc} \leq 0.11$ in Tevatron Run I. These will reduce to $\zeta_{tu} \leq 0.0021$, $\zeta_{tc} \leq 0.0046$ after the first LHC run with a luminosity of 10 fb^{-1} . In the following we investigate in detail what can be learned from Zt and γt production at Tevatron.

Zt production. In general this process manifests as a five fermion final state. The relatively low statistics available at Tevatron makes the $\nu\bar{\nu}jjb$ channel the most interesting mode due to its branching ratio, 13%. The $j\bar{j}l\nu b$ channel with a branching ratio of 15% gives less precise results due to its larger background. We will only consider $l = e, \mu$ throughout this Letter, but with an efficient τ identification the total branching ratio increases by a factor $\sim 3/2$, improving the significance of this channel. The l^+l^-jjb mode has a smaller branching ratio and the hadronic decay channel $jjjjb$ a larger background, whereas the three-neutrino channel $\nu\bar{\nu}l\nu b$

has both a smaller branching ratio and a larger background. On the other hand, the $b\bar{b}l\nu b$ and $l^+l^-\nu b$ modes have smaller branching ratios and backgrounds, and become the most interesting channels at Tevatron with very high luminosity and at the LHC. The three charged lepton signal is also characteristic of some gauge mediated supersymmetry breaking (GMSB) models [13]. However, if the origin of such a signal is a top FCN coupling, the other decay channels must show up in the ratio dictated by the Z and W decay rates.

jjb \cancel{E}_T signal. We discuss first the $\nu\bar{\nu}jjb$ mode which is the best way of measuring the Ztu vertex. We will consider both γ_μ and $\sigma_{\mu\nu}$ terms, but we will assume only one at a time to be nonzero¹. The samples are generated using the exact matrix element for the s- and t-channel diagrams $gu \rightarrow Zt \rightarrow ZWb \rightarrow \nu\bar{\nu}q\bar{q}'b$. The SM diagrams contributing to $gu \rightarrow ZWb$ are much smaller in the phase space region of interest and suppressed by small mixing angles, and we neglect them here. We assume all fermions massless except the top quark. In order to estimate the background we have evaluated four other processes: (i) $Zjjj$ production using VECBOS [14] modified to include energy smearing and kinematical cuts; (ii) $Zb\bar{b}j$ production, which is much smaller and only important at Run II when we use b tagging; (iii) the process $gb \rightarrow Wt \rightarrow WWb \rightarrow l\bar{\nu}q\bar{q}'b$, where l is missed, and (iv) $t\bar{t}$ production with $\bar{t}(t) \rightarrow l\nu b$, with l and b missed and $t(\bar{t}) \rightarrow q\bar{q}'b$. We include throughout this Letter a K factor equal to 1.2 for all processes [15], except for $t\bar{t}$ production where we use $K = 1.34$ [16]. We use MRST structure functions set A [17] with $Q^2 = \hat{s}$. The cross section for both γ_μ or $\sigma_{\mu\nu}$ couplings is 235 fb at $\sqrt{s} = 1.8$ TeV, assuming the present upper limits, $X_{tu} = 0.84$ and $\kappa_{tu} = 0.78$. For $\sqrt{s} = 2$ TeV, the cross sections increase to 358 and 370 fb, respectively. After generating signals and backgrounds we imitate the experimental conditions with a Gaussian smearing of the lepton (l), photon (γ) and jet (j) energies,

$$\begin{aligned}\frac{\Delta E^{l,\gamma}}{E^{l,\gamma}} &= \frac{20\%}{\sqrt{E^{l,\gamma}}} \oplus 2\%, \\ \frac{\Delta E^j}{E^j} &= \frac{80\%}{\sqrt{E^j}} \oplus 5\%,\end{aligned}\tag{4}$$

where the energies are in GeV and the two terms are added in quadrature. (For simplicity we assume that the energy smearing for muons is the same as for electrons.) We then apply detector cuts on transverse momenta p_T , pseudorapidities η and distances in (η, ϕ) space ΔR :

$$p_T^{l,j} \geq 10 \text{ GeV}, \quad p_T^\gamma \geq 16 \text{ GeV}, \quad |\eta^{l,j,\gamma}| \leq 2, \quad \Delta R_{jj,lj,\gamma l,\gamma j} \geq 0.4.\tag{5}$$

¹To be definite we fix the ratio $X_{tu}^L/X_{tu}^R = 4/3$.

For the Wt and $t\bar{t}$ backgrounds, we estimate in how many events we miss the charged lepton and the b jet demanding that their momenta and pseudorapidities satisfy $p_T < 10$ GeV or $|\eta| > 3$.

For the events to be triggered, we require both the signal and background to fulfil at least one of the following trigger conditions:

- one jet with $p_T \geq 100$ GeV,
- one charged lepton with $p_T \geq 20$ GeV and $|\eta| \leq 1$,
- one photon with $p_T \geq 16$ GeV and $|\eta| \leq 1$,
- missing energy $\cancel{E}_T \geq 35$ GeV and one jet with $p_T \geq 50$ GeV,
- four jets (including leptons and photons) with $p_T \geq 15$ GeV and $\sum p_T \geq 125$ GeV.

Finally, for the Tevatron Run II analysis we will take advantage of the good b tagging efficiency $\sim 60\%$ [18] to require a tagged b jet in the final state. There is also a small probability $\sim 1\%$ that a jet which does not result from the fragmentation of a b quark is misidentified as a b jet [19]. b tagging is then implemented in the Monte Carlo routines taking into account all possibilities of b (mis)identification and requiring *only* one b jet. This reduces the signal and the Wt and $t\bar{t}$ backgrounds by a factor of ~ 0.6 , the largest background $Zjjj$ by ~ 0.03 and the $Zb\bar{b}j$ background by ~ 0.48 . b tagging is not convenient at Run I because the number of signal events and the b -tagging efficiency are small. In Fig. 1 we plot the signal and background distributions for m_t^{rec} , the invariant mass of the three jets, which is the reconstructed mass of the top quark for the signal. Obviously in this case m_t^{rec} is not exactly the top mass, because the t quark is not necessarily on-shell. Besides, we have also simulated the detector by smearing the energy. Both effects are in fact comparable. Obviously, the m_t^{rec} distribution for the Wt and $t\bar{t}$ backgrounds peaks also around m_t . In Fig. 2 we plot the cross section as a function of M_W^{rec} , the reconstructed W boson mass. When we use b tagging, M_W^{rec} is the invariant mass of the other two jets. If the b is not tagged, M_W^{rec} is defined as the two-jet invariant mass closest to the W mass. In this case the third jet is indirectly assigned to a b . M_W^{rec} equals M_W for the signal and the Wt and $t\bar{t}$ backgrounds. Another useful variable to discriminate between signal and background is the total transverse energy H_T in Fig. 3, which is defined as the scalar sum of the p_T 's of all jets plus \cancel{E}_T . In Fig. 4 we plot the \cancel{E}_T distribution to show that the possible trigger inefficiency will not change significantly our results.

To enhance the signal to background ratio we apply different sets of cuts on m_t^{rec} , M_W^{rec} , H_T in Runs I and II, and also on p_T^b , the transverse momentum of

the b quark, p_t^{\min} , the minimum transverse momentum of the jets and ΔR_{jj}^{\min} , the minimum ΔR between jets (see Table 1). The total number of events for Runs I and II with integrated luminosities of 109 pb^{-1} and 2 fb^{-1} , respectively, are collected in Table 2, using for the signals $X_{tu} = 0.84$ and $\kappa_{tu} = 0.78$. We observe that the kinematical cuts in Table 1 are very efficient to reduce the $Zjjj$ and $Zbbj$ backgrounds, but they do not affect Wt and $t\bar{t}$. These are in practice irreducible and limit the usefulness of this decay channel to moderate energies and luminosities. To derive upper bounds on the coupling constants we use the prescriptions in Ref. [20]. These are more adequate than naïve Poisson statistics when the number of background events is small, as happens in our case. (Notice that these prescriptions are similar to those applied in Ref. [3] to obtain the bounds $\text{Br}(t \rightarrow Zq) \leq 0.33$ and $\text{Br}(t \rightarrow \gamma q) \leq 0.032$.) Unless otherwise stated, all bounds will be calculated at 95% C. L. This decay channel gives, if no signal is observed, $X_{tu} \leq 0.690$, $\kappa_{tu} \leq 0.596$ after Run I and $X_{tu} \leq 0.180$, $\kappa_{tu} \leq 0.155$ after Run II. The expected limit from top decay in Run II is $X_{tu} \leq 0.225$ [8]. Scaling this value with the Run I limits in Eq. 3 we estimate $\kappa_{tu} \leq 0.208$ at Run II.

Variable	Run I	Run II
m_t^{rec}	155–200	155–200
M_W^{rec}	70–95	65–95
H_T	> 180	> 160
p_T^b		> 20
p_T^{\min}	> 20	
ΔR_{jj}^{\min}	> 0.6	

Table 1: Kinematical cuts for the $\nu\bar{\nu}jjb$ decay channel. The masses, energies and momenta are in GeV. At Run II we also use b tagging.

This process also constrains the strong anomalous top coupling ζ_{tu} . Again there are two s- and t-channel diagrams contributing to the signal and a similar analysis gives $\zeta_{tu} \leq 0.316$ after Run I and $\zeta_{tu} \leq 0.0824$ after Run II. These bounds are weaker than the top decay limits $\zeta_{tu} \leq 0.15$ and $\zeta_{tu} \leq 0.04$, respectively [6], and than the limits from jt production $\zeta_{tu} \leq 0.029$ and $\zeta_{tu} \leq 0.009$ [12]. One may wonder if it is sensible to use the same cuts for the Z anomalous terms γ_μ and $\sigma_{\mu\nu}$ and for the strong $\sigma_{\mu\nu}$ terms. The characteristic q^ν behaviour differentiates the $\sigma_{\mu\nu}$ from the γ_μ terms and manifests differently if the vertex involves the initial gluon or the final Z boson. However, this makes little difference for Tevatron energies and we do not distinguish among the three cases.

	Run I		Run II	
	before cuts	after cuts	before cuts	after cuts
$Zt(\gamma_\mu)$	16.0	10.8	261	235
$Zt(\sigma_{\mu\nu})$	18.1	12.4	306	274
$Zjjj$	281	7.2	199	5.2
$Zb\bar{b}j$	4.0	0.2	74.1	2.3
Wt	0.2	0.1	3.5	3.4
$t\bar{t}$	0.9	0.6	10.6	9.9

Table 2: Number of $\nu\bar{\nu}jjb$ events before and after the kinematical cuts in Table 1 for the Zt signal and backgrounds. We use $X_{tu} = 0.84$ and $\kappa_{tu} = 0.78$.

ljjbE_T signal. The $jjl\nu b$ decay channel analysis is carried out in a completely analogous way. We consider $Wjjj$ and $Wb\bar{b}j$ production, which we evaluate with VECBOS, and Wt and $t\bar{t}$ production, with a b quark missing in the latter, as backgrounds to our signal (for other single top production processes see Ref. [21]). To reconstruct the Z boson mass M_Z^{rec} we use in Run I the two-jet invariant mass closest to the Z mass, assigning the remaining jet to the b . In Run II we require *only* one tagged b defining M_Z^{rec} as the invariant mass of the other two jets². We make the hypothesis that all missing energy comes from a single neutrino with $p^\nu = (E^\nu, \not{p}_T, p_L^\nu)$, and \not{p}_T the missing transverse momentum. Using $(p^l + p^\nu)^2 = M_W^2$ we find two solutions for p^ν , and we choose that one making the reconstructed top mass $m_t^{\text{rec}} \equiv \sqrt{(p^l + p^\nu + p^b)^2}$ closest to m_t . The complete set of cuts for Runs I and II is gathered in Table 3. In addition we require $E_T > 5$ GeV to ensure that the top mass reconstruction is meaningful. The number of events before and after cuts is given in Table 4, taking again for the signals $X_{tu} = 0.84$ and $\kappa_{tu} = 0.78$. We observe that although the $Wjjj$ background is one order of magnitude larger than the $Zjjj$ background of the previous signal, the cuts are more effective. This is so in part because m_t^{rec} and M_Z^{rec} depend on different momenta, whereas in the $\nu\bar{\nu}jjb$ mode $(m_t^{\text{rec}})^2 = (M_W^{\text{rec}})^2 + 2p^W \cdot p^b$. In Run I without b tagging $Wjjj$ is the main background, but at Run II all backgrounds are in practice comparable. As the only way to get rid of Wt and $t\bar{t}$ is distinguishing $Z \rightarrow jj$ from $W \rightarrow jj$, we require $M_Z^{\text{rec}} > 90$ GeV in this Run. The cuts in Table 3 are a compromise to reduce the

²Requiring only one tagged b reduces the signal because the Z boson decays to $b\bar{b}$ 15% of the time. In this case we have then three b 's but we require only one tagged b . The case with more than one tagged b will be discussed in Ref. [2].

different backgrounds keeping at the same time the signal as large as possible. Thus if no signal is observed, we obtain from Table 4 $X_{tu} \leq 0.838$, $\kappa_{tu} \leq 0.705$ after Run I and $X_{tu} \leq 0.275$, $\kappa_{tu} \leq 0.222$ after Run II.

The bounds on ζ_{tu} are again not competitive with those derived from top decays and jt production. In this channel we find $\zeta_{tu} \leq 0.374$ (0.119) after Run I (II).

Variable	Run I	Run II
M_Z^{rec}	80–105	90–110
m_t^{rec}	155–200	150–200
H_T	> 240	> 240
p_T^b	> 20	
$\Delta R_{jj}^{\text{min}}$	> 0.5	> 0.6

Table 3: Kinematical cuts for the $j\bar{j}l\nu b$ decay channel. The masses, energies and momenta are in GeV. At Run II we also use b tagging.

	Run I		Run II	
	before cuts	after cuts	before cuts	after cuts
$Zt(\gamma_\mu)$	17.9	9.9	259	77.2
$Zt(\sigma_{\mu\nu})$	19.7	12.0	284	101
$Wj\bar{j}j$	1928	13.3	1282	2.7
$Wb\bar{b}j$	41.6	0.2	421	1.0
Wt	4.6	0.8	86.6	5.5
$t\bar{t}$	15.2	2.7	226	2.8

Table 4: Number of $j\bar{j}l\nu b$ events before and after the kinematical cuts in Table 3 for the Zt signal and backgrounds. We use $X_{tu} = 0.84$ and $\kappa_{tu} = 0.78$.

γt production. This process gives a final state of a photon and three fermions. In this case there are no γ_μ terms as required by gauge invariance. Depending whether the W decays into leptons or hadrons, we have the signal $\gamma l\nu b$ or $\gamma j\bar{j}b$. As in Zt production, we only consider $l = e, \mu$, and again a good τ identification will improve our results. Then the leptonic mode has a branching ratio of 21%, and the hadronic mode 67.9%. However, the leptonic mode has a small background from the SM γWj production, whereas the hadronic one has a huge background from $\gamma j\bar{j}j$

production.

$\gamma lb\cancel{E}_T$ signal. This signal is again generated using the exact matrix element for the two s- and t-channel diagrams $gu \rightarrow \gamma t \rightarrow \gamma Wb \rightarrow \gamma l\nu b$ and $\lambda_{tu} = 0.26$. Here we have also neglected the SM diagrams $gu \rightarrow \gamma Wb$ which are also negligible in the phase space of interest. The main SM background is γWj production. We consider $gq_u \rightarrow \gamma Wq_d$, $gq_d \rightarrow \gamma Wq_u$ and $q_u\bar{q}_d \rightarrow \gamma Wg$, with $q_u = u, c$ and $q_d = d, s$ (plus the charge conjugate processes), with the jet misidentified as a b . The true b production from initial u and c quarks is suppressed by the Cabibbo-Kobayashi-Maskawa matrix elements $|V_{ub}|^2$ and $|V_{cb}|^2$, respectively, and is negligible. To evaluate the background we have first calculated the matrix element for $gq_u \rightarrow \gamma Wq_d$, including the eight SM diagrams, decaying afterwards the W leptonically. The matrix elements for the other two processes can be obtained by crossing symmetry. Our result for γWj production at Tevatron Run I agrees with the cross-section obtained in Ref. [22]. We use the same detector and trigger cuts as for Zt production. We also take advantage of b tagging in Run II to reduce the background (in this process there is only one jet).

To improve the signal to background ratio we perform kinematical cuts on m_t^{rec} , which is defined as in the $jjl\nu b$ channel for Zt production (see Fig. 5). We also require large H_T (Fig. 6), p_T^γ (Fig. 7) and E^γ . The complete set of cuts for Runs I and II is gathered in Table 5, where we have also required $\Delta R_{\gamma W} > 0.4$, and the number of events in Table 6. Notice that the cuts for Run II are less restrictive than for Run I. This is so because b tagging alone reduces drastically the background in Run II. In Run I the statistics is too low to improve the top decay bound, and we only get $\lambda_{tu} \leq 0.30$. However with the increase in energy and luminosity in Run II the characteristic behaviour of the $\sigma_{\mu\nu}$ coupling starts to manifest and the bound obtained from this process, $\lambda_{tu} \leq 0.066$, is better than the limit from top decays, $\lambda_{tu} \leq 0.09$ [9].

Variable	Run I	Run II
m_t^{rec}	150–205	140–210
H_T	> 180	> 160
p_T^γ	> 40	> 30
E^γ	> 50	

Table 5: Kinematical cuts for the $\gamma l\nu b$ decay channel. The masses, energies and momenta are in GeV. At Run II we also use b tagging.

This process also constrains the strong top FCN vertex. Two s- and t-channel diagrams contribute to $gu \rightarrow \gamma t$ production. Evaluating the exact matrix element

	Run I		Run II	
	before cuts	after cuts	before cuts	after cuts
γt	4.2	3.5	68.4	63.5
γW_{qu}	10.3	0.5	2.5	0.3
γW_{qd}	10.3	0.4	2.6	0.3
γWg	39.4	1.3	8.5	0.7

Table 6: Number of $\gamma l \nu b$ events before and after the kinematical cuts in Table 5 for the γt signal and backgrounds. We use $\lambda_{tu} = 0.26$.

and proceeding as before we obtain $\zeta_{tu} \leq 0.11$ after Run I and $\zeta_{tu} \leq 0.020$ after Run II. These bounds are better than those obtained from top decay, but they are still weaker than the bounds from tj production.

γjjb signal. This decay channel has a larger branching ratio than the previous one, but also a larger background. In order to evaluate it, we have modified VECBOS to produce photons instead of Z bosons. This is done introducing a ‘photon’ with a small mass $m_\gamma = 0.1$ GeV and substituting the Z couplings by the photon couplings everywhere. The total width of such ‘photon’ is calculated to be $\Gamma_\gamma = 1.73 \cdot 10^{-3}$ GeV, with an e^+e^- branching ratio equal to 0.15. We have checked that the results are the same for a heavier ‘photon’ with $m_\gamma = 1$ GeV and $\Gamma_\gamma = 1.73 \cdot 10^{-2}$ GeV. After detector and trigger cuts, the total number of signal events is 12 at Run I, while the background is huge, 65705 events. However, with b tagging at Run II we still can derive a competitive bound on the electromagnetic anomalous coupling. The reconstruction of the top and the W mass proceeds as in the $\nu \bar{\nu} jjb$ signal. The cuts for γjjb are summarized in Table 7, with p_T^{\max} the maximum transverse momentum of the three jets. The number of events before and after cuts can be read from Table 8 (for the signal we use $\lambda_{tu} = 0.26$). In this case we derive a bound $\lambda_{tu} \leq 0.088$ similar to that expected from top decays, but worse than the one obtained in the $\gamma l \nu b$ channel.

This channel also allows to constrain the strong anomalous coupling ζ_{tu} . Proceeding as before we derive the bound $\zeta_{tu} \leq 0.048$ after Run II.

In summary, we have shown that Zt and γt production at large hadron colliders provides a sensitive probe for anomalous FCN top couplings. At Tevatron energies these processes are sensitive only to Vtu couplings. For Zt production the most interesting channels are those with $Z \rightarrow \nu \bar{\nu}$ and $W \rightarrow q \bar{q}'$, and $Z \rightarrow q \bar{q}$ and $W \rightarrow l \nu$. For γt production, both channels $W \rightarrow q \bar{q}'$ and $W \rightarrow l \nu$ are significant. The limits

Variable	Run II
m_t^{rec}	160–200
M_W^{rec}	65–95
H_T	> 240
p_T^γ	> 75
E^γ	> 100
p_T^{max}	> 50
$\Delta R_{jj}^{\text{min}}$	> 0.6

Table 7: Kinematical cuts for the γjjb decay channel. The masses, energies and momenta are in GeV. In this Run we use b tagging.

	Run II	
	before cuts	after cuts
γt	192	89.9
γjjj	54290	19.1

Table 8: Number of γjjb events before and after the kinematical cuts in Table 7 for the γt signal and background. We use $\lambda_{tu} = 0.26$

which can be obtained from these signals are quoted in Table 9, together with present and future bounds from top decays and jt production.

With the increase of the center of mass energy and luminosity at the LHC, the $l^+l^-\nu b$ and $b\bar{b}l\nu b$ channels will provide the most precise bounds on X_{tu} and κ_{tu} , while the $\gamma l\nu b$ channel will give the strongest bound on λ_{tu} and ζ_{tu} . At the same time, Zt and γt production from sea c quarks becomes larger and similar bounds to those from top decays can be obtained. This is the subject of Ref. [2].

Acknowledgements

We thank W. Giele for helping us with VECBOS and J. Fernández de Trocóniz and I. Efthymiopoulos for discussions on Tevatron and LHC triggers. We have also benefited from discussions with F. Cornet, M. Mangano and R. Miquel. This work was partially supported by CICYT under contract AEN96–1672 and by the Junta

Signal	Run I				Run II			
	X_{tu}	κ_{tu}	λ_{tu}	ζ_{tu}	X_{tu}	κ_{tu}	λ_{tu}	ζ_{tu}
$\nu\bar{\nu}jjb$	0.69	0.60	—	0.32	0.18	0.15	—	0.082
$jjl\nu b$	0.84	0.71	—	0.37	0.28	0.22	—	0.12
$\gamma l\nu b$	—	—	0.30	0.11	—	—	0.066	0.020
γjjb	—	—	—	—	—	—	0.088	0.048
Top decay	0.84	0.78	0.26	0.15	0.23	0.21	0.09	0.04
jt production	—	—	—	0.029	—	—	—	0.009

Table 9: Summary of the bounds on the anomalous top couplings in Eqs. (1), (3) obtained from the main decay channels in single top production in association with a Z boson or a photon at Tevatron. For comparison we also quote the limits from top decay and single top production plus a jet existing in the literature. We use dashes to indicate that the process does not constrain the coupling at tree level. In Run I the γjjb signal gives no significant bound.

de Andalucía, FQM101.

References

- [1] C. Caso *et al.*, European Phys. Journal **C3**, 1 (1998)
- [2] F. del Aguila and J. A. Aguilar-Saavedra, UG-FT-100/99
- [3] F. Abe *et al.*, Phys. Rev. Lett. **80**, 2525 (1998)
- [4] C. Burgess and H. J. Schnitzer, Nucl Phys. **B228**, 464 (1983); W. Buchmüller and D. Wyler, Nucl. Phys. **B268**, 621 (1986); C. N. Leung, S. T. Love and S. Rao, Z. Phys. **C31**, 433 (1986); R. D. Peccei, S. Peris and X. Zhang, Nucl. Phys. **B349**, 305 (1991); R. Escribano and E. Masso, Nucl. Phys. **B429**, 19 (1994)
- [5] F. del Aguila, J. A. Aguilar-Saavedra and R. Miquel, Phys. Rev. Lett. **82**, 1628 (1999); see also F. del Aguila and J. A. Aguilar-Saavedra, UG-FT-99/99, hep-ph/9906461
- [6] T. Han, K. Whisnant, B.-L. Young and X. Zhang, Phys. Lett. **B385**, 311 (1996)
- [7] DELPHI Collaboration, S. Andringa *et al.*, DELPHI 98-70 CONF 138

- [8] T. Han, R. D. Peccei and X. Zhang, Nucl. Phys. **B454**, 527 (1995)
- [9] T. Han, K. Whisnant, B.-L. Young and X. Zhang, Phys. Rev. **D55**, 7241 (1997)
- [10] T. Han and J. L. Hewett, hep-ph/9811237, Phys. Rev. **D** (in press)
- [11] S. Bar-Shalom and J. Wudka, hep-ph/9905407
- [12] T. Han, M. Hosch, K. Whisnant, B.-L. Young and X. Zhang, Phys. Rev. **D58**, 073008 (1998)
- [13] H. Baer, P. G. Mercadante, X. Tata and Y. Wang, hep-ph/9903333 and references there in
- [14] F. Berends, H. Kuijf, B. Tausk and W. Giele, Nucl. Phys. **B357**, 32 (1991)
- [15] R. Hamberg, W.L. van Neerven and T. Matsuura, Nucl. Phys. **B359**, 343 (1991)
- [16] S. Frixione, M. Mangano, P. Nason and G. Ridolfi, hep-ph/9702287, to be published in Heavy Flavours II, eds. A.J. Buras and M. Lindner, World Scientific
- [17] A. D. Martin, R. G. Roberts, W. J. Stirling and R. S. Thorne, Eur. Phys. J. **C4**, 463 (1998)
- [18] F. Abe *et al.*, Phys. Rev. Lett. **80**, 2779 (1998)
- [19] F. Abe *et al.*, Phys. Rev. **D50**, 2966 (1994)
- [20] G. J. Feldman and R. D. Cousins, Phys. Rev. **D57**, 3873 (1998)
- [21] T. Stelzer, Z. Sullivan and S. Willenbrock, Phys. Rev. **D58**, 094021 (1998)
- [22] V. Barger, T. Han, J. Ohnemus and D. Zeppenfeld, Phys. Rev. **D41**, 2782 (1990); for LHC calculations see also U. Baur, E. W. N. Glover and J. J. van der Bij, Nucl. Phys. **B318**, 106 (1989)

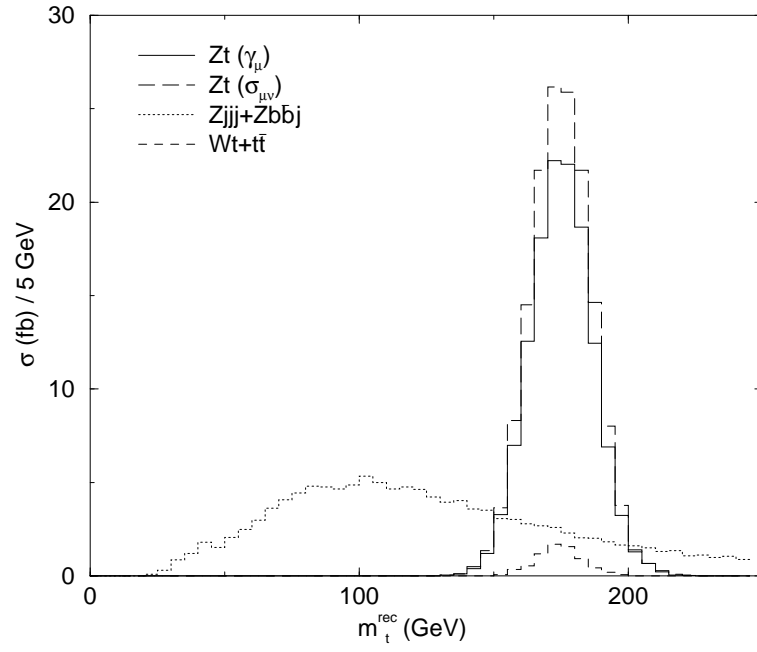


Figure 1: Reconstructed top mass m_t^{rec} distribution before kinematical cuts for the $\nu\bar{\nu}jjb$ signal and backgrounds in Tevatron Run II.

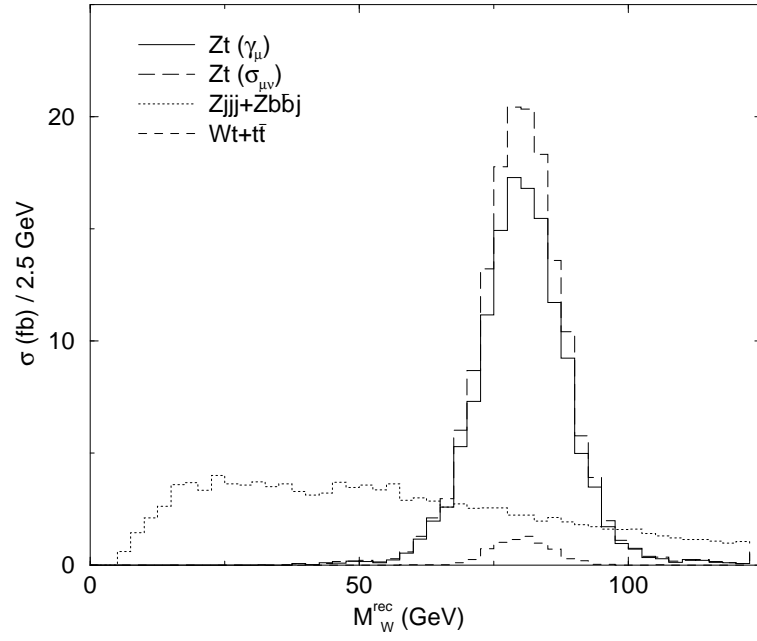


Figure 2: Reconstructed W mass M_W^{rec} distribution before kinematical cuts for the $\nu\bar{\nu}jjb$ signal and backgrounds in Tevatron Run II.

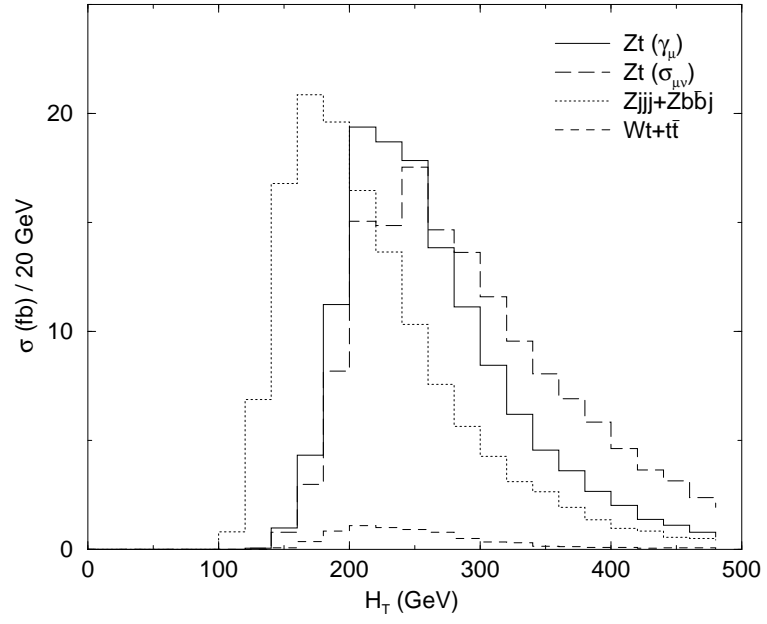


Figure 3: Total transverse energy H_T distribution before kinematical cuts for the $\nu\bar{\nu}jjb$ signal and backgrounds in Tevatron Run II.

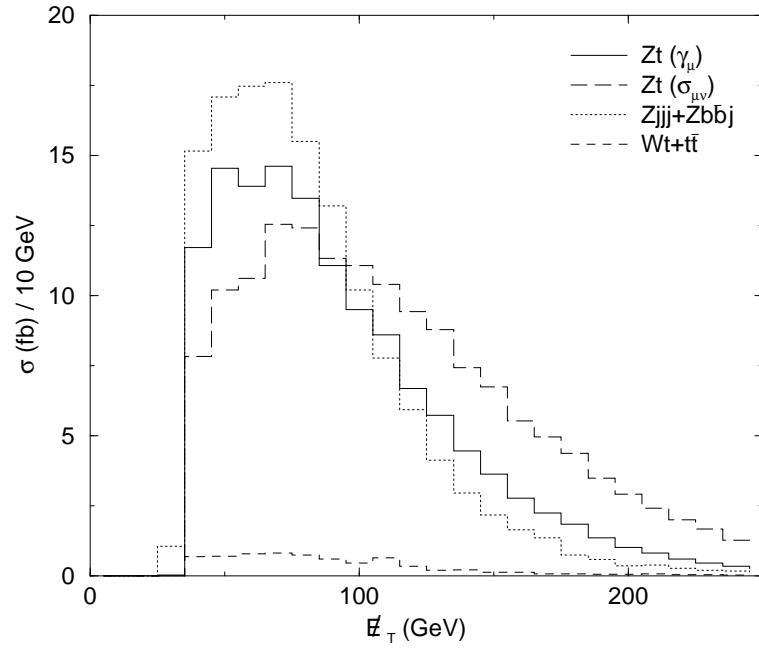


Figure 4: Missing transverse energy E_T distribution before kinematical cuts for the $\nu\bar{\nu}jjb$ signal and backgrounds in Tevatron Run II.

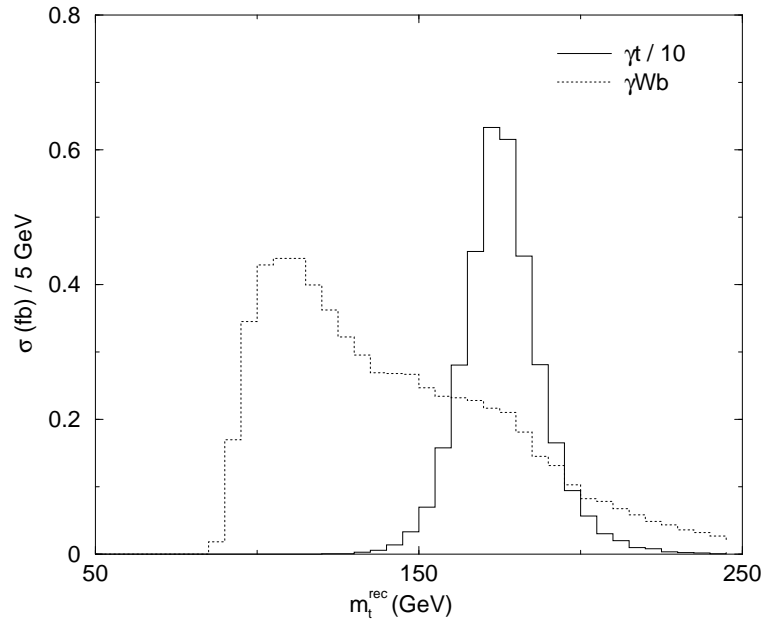


Figure 5: Reconstructed top mass m_t^{rec} distribution before kinematical cuts for the $\gamma l \nu b$ signal and background in Tevatron Run II. For comparison the signal distribution has been divided by 10.

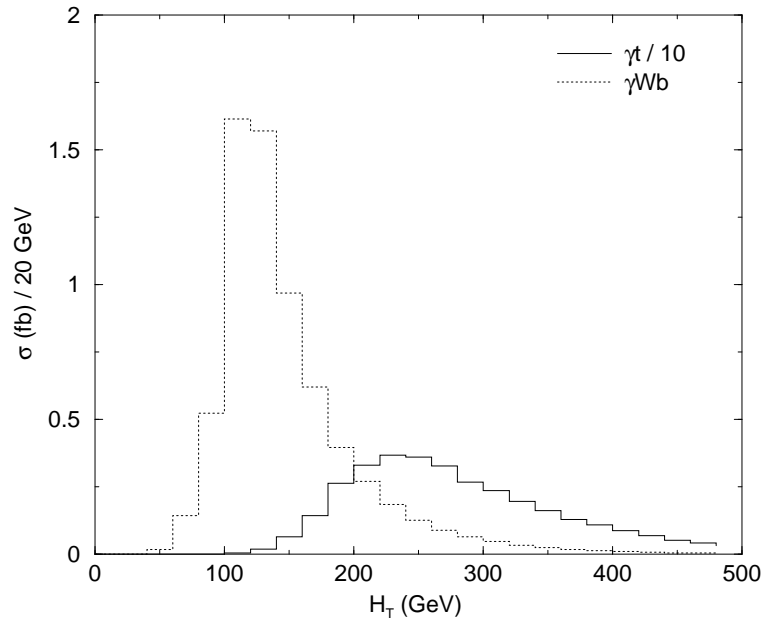


Figure 6: Total transverse energy H_T distribution before kinematical cuts for the $\gamma l \nu b$ signal and background in Tevatron Run II. For comparison the signal distribution has been divided by 10.

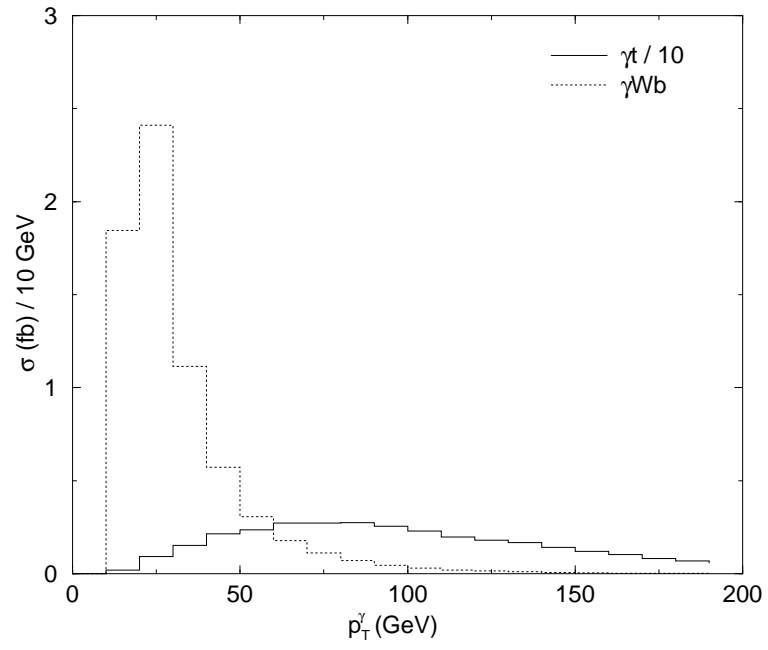


Figure 7: Photon transverse momentum p_T^γ distribution before kinematical cuts for the $\gamma l \nu b$ signal and background in Tevatron Run II. For comparison the signal distribution has been divided by 10.